

Study of the $^{24}\text{Mg}(^3\text{He}, p)^{26}\text{Al}$ Reaction*

R. R. Betts and H. T. Fortune

Department of Physics, University of Pennsylvania, Philadelphia, Pennsylvania 19104

and

D. J. Pullen

Department of Physics and Applied Physics, Lowell Technological Institute, Lowell, Massachusetts 01854

(Received 5 June 1972)

The nuclear structure of ^{26}Al has been studied by means of the $^{24}\text{Mg}(^3\text{He}, p)$ reaction at an incident energy of 18 MeV. 65 levels below 7 MeV in excitation were observed with an energy resolution of 18 keV. Systematics of the angular-distribution shapes allow several assignments of the angular-momentum transfer, resulting in some new spin assignments. Distorted-wave calculations have been performed for those states previously thought to be well described in terms of pure two-particle Nilsson configurations relative to a ^{24}Mg core.

I. INTRODUCTION

The present study forms part of a systematic investigation of the $(^3\text{He}, p)$ reaction on even-even targets in the $2s-1d$ shell.¹⁻⁴ Firstly, we seek to establish the systematics of the reaction mechanism and to test the methods of performing distorted-wave calculations. As in a similar study of the $^{20}\text{Ne}(^3\text{He}, p)$ reaction,² this aim is accomplished by using transitions to states whose properties have previously been established by other means. The knowledge thus obtained can then be applied to other states in order to obtain new information on the structure of these states.

The results for the $^{24}\text{Mg}(^3\text{He}, p)^{26}\text{Al}$ reaction are reported herein. The energy levels of ^{26}Al below 6.9 MeV in excitation have been previously established by means of the $^{27}\text{Al}(^3\text{He}, \alpha)$ and the $^{24}\text{Mg}(^3\text{He}, p)$ reactions, both performed at a bombarding energy of 5.8 MeV by Hinds and Middleton.⁵

Spins and parities have been assigned to some of the levels below 4.5 MeV from the $^{24}\text{Mg}(^3\text{He}, p\gamma)$ studies of Bissinger, Quin, and Chagnon^{6,7} and from the $^{25}\text{Mg}(p, \gamma)$ studies of Häusser *et al.*^{8,9} The reactions $^{25}\text{Mg}(^3\text{He}, d)^{26}\text{Al}$ and $^{25}\text{Mg}(d, n)^{26}\text{Al}$ have yielded additional information^{10,11} for several states. Some information on spins and parities is available for all states below 4.0 MeV.

Theoretical interpretations of the level scheme of ^{26}Al have been presented by several authors. Horvat, Kump, and Povh¹² have discussed the low-lying levels in terms of the simple Nilsson model, as have Weidinger *et al.*¹⁰ in connection with their study of the $^{25}\text{Mg}(^3\text{He}, d)$ reaction. Bouten, Elliot, and Pullen¹³ presented results of an intermediate-coupling calculation for ^{26}Al in their discussion of this model in the $2s-1d$ shell. The effect of Corio-

lis coupling on the Nilsson Hamiltonian in this mass region has been discussed in detail by Wasielewski and Malik.¹⁴ These authors, however, published only qualitative results for ^{26}Al .

II. EXPERIMENTAL METHOD

The principal experiment was performed at an incident energy of 18 MeV with subsidiary measurements at 11 and 19.5 MeV. The target consisted of $30 \mu\text{g}/\text{cm}^2$ of ^{24}Mg metal (99.96% enrichment) backed by a $100\text{-}\mu\text{g}/\text{cm}^2$ Au foil. Gold rather than carbon was chosen for the target backing in order to minimize contaminant groups arising from the $(^3\text{He}, p)$ reaction on ^{12}C and ^{13}C . The target was bombarded with $^3\text{He}^{++}$ ions from the University of Pennsylvania tandem accelerator. The beam current was kept below $0.3 \mu\text{A}$ in order to avoid evaporation of the Mg.

The target thickness was continually monitored by observing the elastically scattered beam particles in a silicon surface-barrier detector mounted at $37\frac{1}{2}^\circ$ to the beam direction. No deterioration of the target was observed during the course of the experiment.

The reaction protons were recorded in Kodak NTB nuclear emulsion plates placed in the focal planes of a multiangle spectrograph. Mylar foil of 0.015-in. thickness was placed in front of the emulsion plates to prevent all other charged particles from being detected. The proton energies corresponding to states in ^{26}Al were calculated for at least 8 angles from the 18-MeV exposure using the known magnet calibration.¹⁵ These, together with the beam energies calculated from the positions of the strong contaminant groups arising from C and O allowed extraction of Q values for

the ^{26}Al states. The present experiment yielded a Q_0 value of 5922 ± 8 keV, in good agreement with the value of 5920 ± 3 keV determined from the masses.¹⁶

III. RESULTS

A proton spectrum obtained at an incident energy of 18 MeV and at a lab angle of $18\frac{3}{4}^\circ$ is shown in Fig. 1. The total charge collected was 4.0 mC. Groups corresponding to states in ^{26}Al are labeled numerically; contaminant groups due to the $(^3\text{He}, p)$ reaction on ^{12}C and ^{16}O are labeled by the final nucleus and level number and are shown shaded. (The presence of C and O is presumably due to carbon buildup and to slight oxidation of the target.)

A total of 65 states below 7 MeV excitation in ^{26}Al have been identified, and their excitation energies are given in Table I in comparison with previous work.¹⁷ Angular distributions of these transitions measured at 18-MeV incident energy are shown in Fig. 2. The angular distribution for the 3722-keV state was also measured at 19.5-MeV incident energy and is displayed in Fig. 3. Distributions for this state and the 3751-keV doublet were in addition measured at 11 MeV and are shown in Fig. 4.

The absolute cross-section scales were determined from the nominal target thickness for the 18- and 19.5-MeV exposures and are believed accurate to $\pm 20\%$. No absolute cross sections were

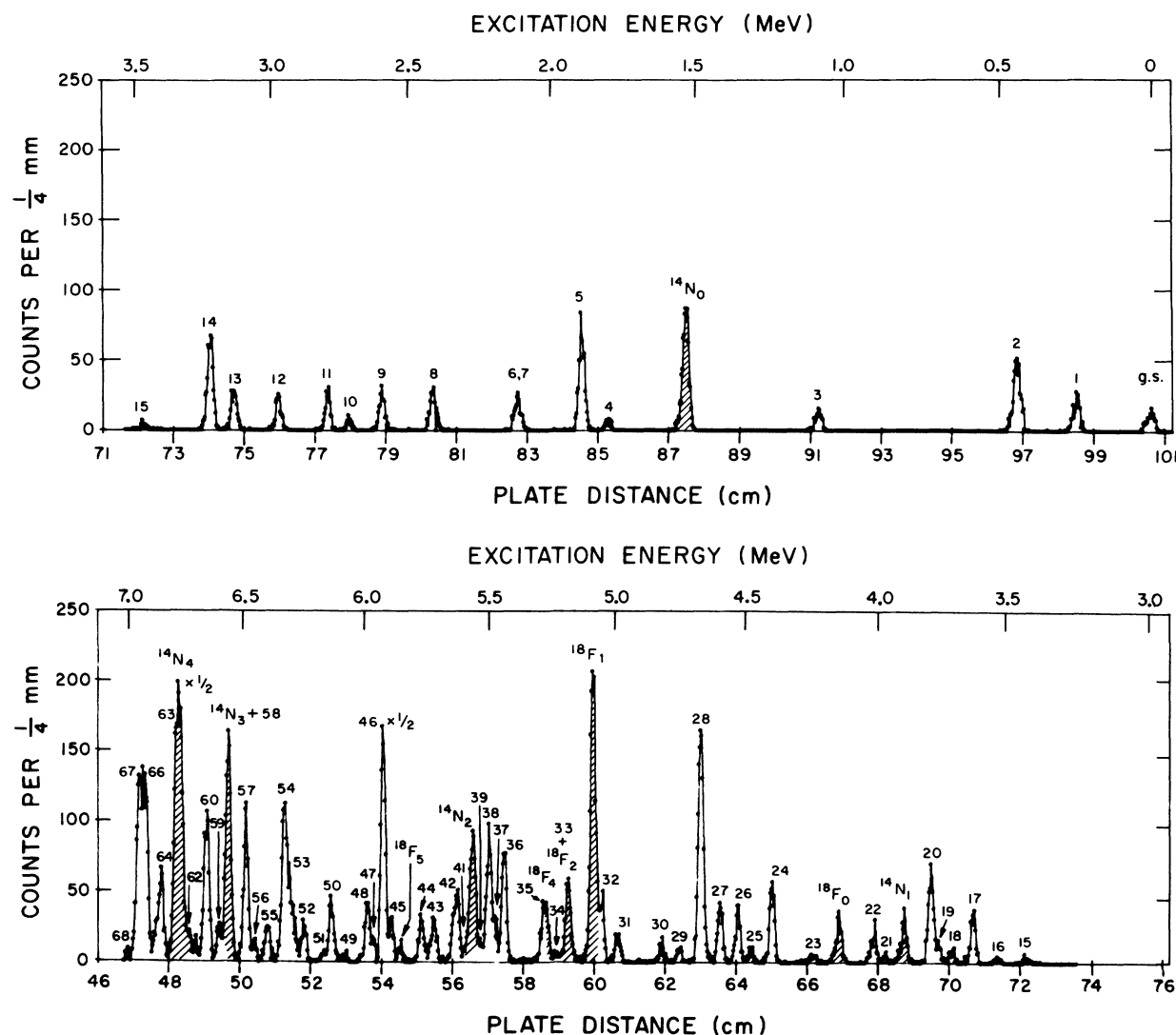


FIG. 1. Proton spectrum from the $^{24}\text{Mg}(^3\text{He}, p)$ reaction obtained at a bombarding energy of 18 MeV and a laboratory angle of 18.75° . Levels in ^{26}Al are labeled numerically. Contaminant groups are shaded and are labeled according to the final nucleus and level number.

TABLE I. Results and spin assignments from the $^{24}\text{Mg}(^3\text{He}, p)^{26}\text{Al}$ reaction.

Level No.	E_x (keV)		$\sigma(\theta)_{\text{max}}$ ($\mu\text{b}/\text{sr}$)	L ($^3\text{He}, p$)	Literature ^c	J^π Assignment
	Present ^a	Literature ^b				
0	0	0	36	(4)	5 ⁺	
1	224	228	250	0	0 ⁺ , $T=1$	
2	414	417	118	2+(4)	3 ⁺	
3	1056	1058	246	0+2	1 ⁺	
4	1763	1759	12	2	2 ⁺	
5	1849	1850	714	0+2	1 ⁺	
6, 7	2072	{2069} {2070} {2072}	167	0+2	{3 ⁺ } {2 ⁺ , $T=1$ } 1	$J^\pi=1^+$
8	2364	2365	54	2	3 ⁺	
9	2545	2545	55	2	3 ⁺	
10	2665	2661	21	(2)	(2, 3) ⁺	
11	2742	2740	43	2	1	$\pi=+$
12	2917	2913	40	2	2 ⁺	
13	3075	3074	82	(2)	(2, 3) ⁺	
14	3162	3159	132	2	2 ⁺ , $T=1$	
15	3408	3405	11	...	5 ⁺	
16	3507	3507	8	...	6 ⁺	
17	3600	3594	54	2	(2, 3) ⁺	
18	3677 ^d	3675	21	...	(2, 3) ⁺	
19	3722	3719	31(53) ^e	0	1	$J^\pi=1^+$
20	3751 ^d	3745	102	0+2	{0 ⁺ , $T=1$ }	Doublet
21	3924	3918	8	...	{(2, 3) ⁺ }	
22	3969	{3950} {3960}	40	(2)	{3, 1} {1, 0}	
23	4192	{4191} {4202}	19	...	3 ⁺ , $T=1$	
24	4345	4342	88	2		(1, 2, 3) ⁺
25	4425	4424	24	4		(3, 4, 5) ⁺
26	4479	4477	82			
27	4546	4541	91			
		4595				
28	4614	4613	563			
29	4704	4699	24			
30	4772	4766	25			
31	4939	4935	41			
32	5000	5002				
33	5148	5126	99			
34	5209	5193	21			
35	5257	5238	40			
36	5406	5390	115			
37	5442	5424	22			
38	5473	5485	174			
		5506				
39	5525	5536	27			
41	5554	5558	14			
42	5593	5580	263			
		5665				
43	5686	5690	159			
44	5741	5715	42			
45	5864	5842	67			
46	5896	5875	595			
47	5935	5910	64			
48	5963	5942	57			
49	6049	6020	10			
50	6100	6080	134			
51	6138	6112	9			
52	6214	6188	168			

TABLE I (Continued)

Level No.	E_x (keV)		$\sigma(\theta)_{\max}$ ($\mu\text{b}/\text{sr}$)	L ($^3\text{He}, p$)	Literature J^π	Assignment
	Present ^a	Literature ^b				
53	6265	6236	105			
54	6294	6260	210			
55	6361	6335	43			
		6351				
56	6417	6388	27			
57	6453	6424	139			
58	6513	6487	19			
59	6565	6544	33			
60	6615	6613	144			
62	6688	6684	92			
63	6738	6727	354			
64	6801	6806	122			
66	6873	6865	187			
67	6899		234			
68	6952		29			

^a All excitation energies possess an estimated uncertainty of ± 8 keV.

^b Reference 17.

^c References 6–11 and 17.

^d Known doublet, Ref. 20.

^e The cross section in parentheses corresponds to that measured at 19.5 MeV. The value of $31 \mu\text{b}/\text{sr}$ measured at 18 MeV is that observed for the second maximum of the angular distribution. The most forward angle was obscured by an impurity group.

measured at 11 MeV.

IV. L VALUES AND SPIN ASSIGNMENTS

The macroscopic selection rules for the ($^3\text{He}, p$) reaction on a 0^+ , $T=0$ target (assuming a direct one-step transfer) are given in Table II. J_f , π_f , and T_f are the spin, parity, and isospin of the final state, L and S are the orbital and spin angular-momentum transfers, and T is the isospin transfer for the np pair.

An inspection of the angular distributions to those states whose spin and parity are known should give the shapes typical of a given L value, providing these states are reached via a direct process. The transitions to the ground state (5^+ ; $L=4+6$) and to the states at 224 keV (0^+ ; $L=0$), 414 keV (3^+ ; $L=2+4$), and 3162 keV (2^+ ; $L=2$) are shown in Fig. 5. Even though an $L=6$ component is allowed by the macroscopic selection rules for the ground-state transition, such a component would involve placing two particles in the $1f-2p$ shell. Since an $(fp)^2$ configuration is unlikely at so low an excitation energy in this nucleus, we expect the ground-state transition to be characterized by pure $L=4$. Thus, in the absence of a known 4^+ state, this transition must serve as our "standard" $L=4$ shape. (See, however, Sec. V.) The remaining angular distributions shown in Fig. 5 are all quite similar to other direct ($^3\text{He}, p$) angu-

lar distributions that have been observed in this mass region.¹⁻⁴ A comparison between the "standard" shapes and those of other transitions enables L values to be assigned for most states below $E_x=4.5$ MeV. In no case is there a conflict between the L value thus obtained and the previously assigned⁶⁻¹¹ spin parity.

In several cases we are able to make a new assignment or to add to the existing information. The level observed at 2072 keV in the present study corresponds to a known triplet of states at excitations of 2069, 2070, and 2072 keV.⁸ The 2069- and 2072-keV members of this triplet have previously been assigned spins of 3 (Ref. 7) and 1 (Ref. 6), respectively, and the 2070-keV state is known to be 2^+ , $T=1$ (Ref. 8). The $L=0$ component in the ($^3\text{He}, p$) angular distribution for the triplet would thus indicate positive parity for the spin 1 member since neither of the other members can be reached via $L=0$. This 1^+ assignment for the 2072-keV state is in agreement with recent work¹⁸ on the β^+ decay of ^{26}Si .

The state at 2742 keV has previously been assigned⁶ $J=1$. The shape of the ($^3\text{He}, p$) angular distribution is characteristic of $L=2$, which would require $J=1, 2$, or 3 and positive parity. If the previous $J=1$ assignment is correct, then these data would yield the unique result $J^\pi=1^+$, $T=0$. However, in the lower half of the $s-d$ shell there exists no established $0^+ \rightarrow 1^+$ transition which is

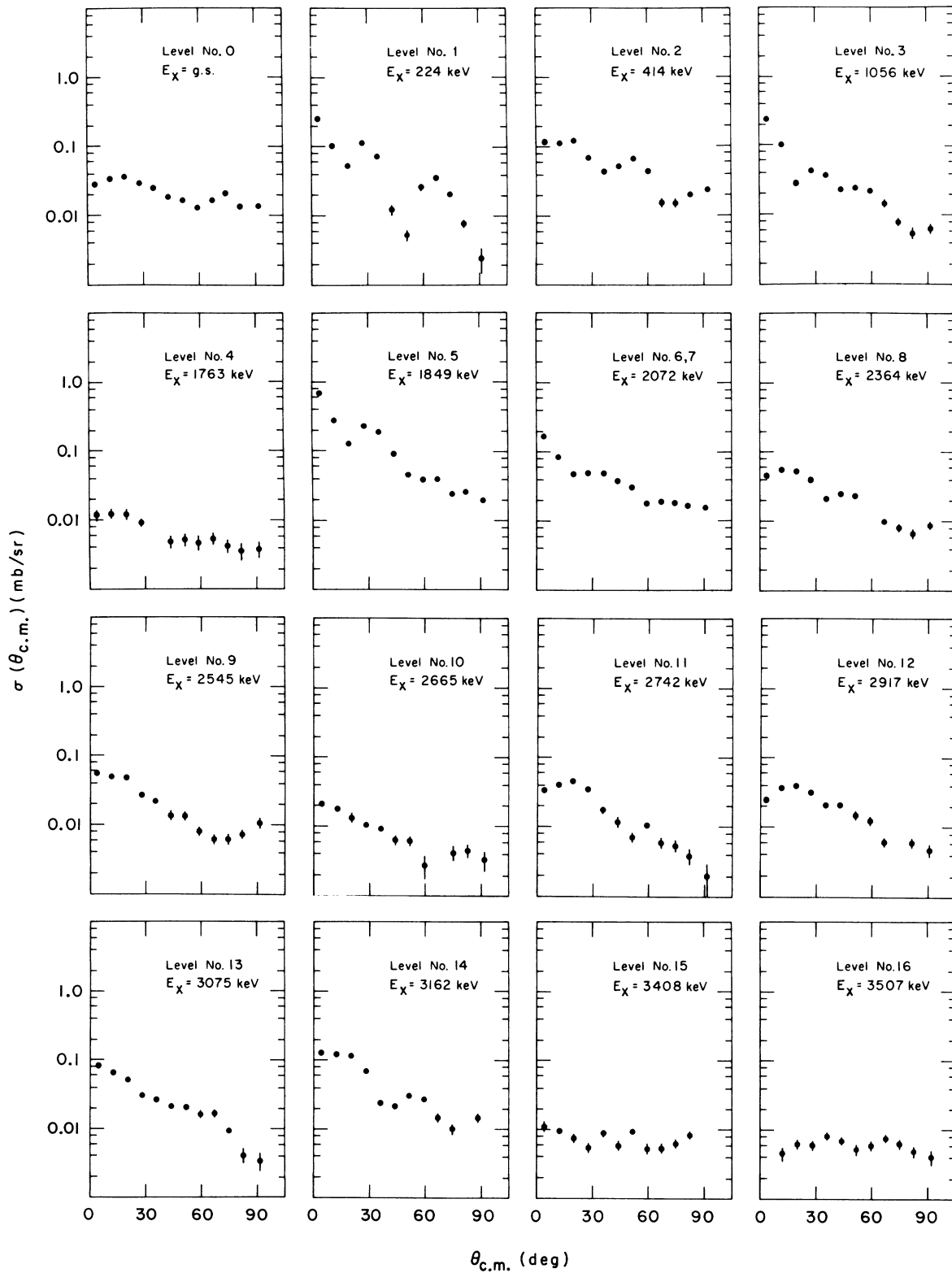


FIG. 2. Angular distributions of the $^{24}\text{Mg}(^3\text{He}, p)^{26}\text{Al}$ reaction at 18-MeV bombarding energy. The absolute cross-section scale is estimated to be accurate to 20%.

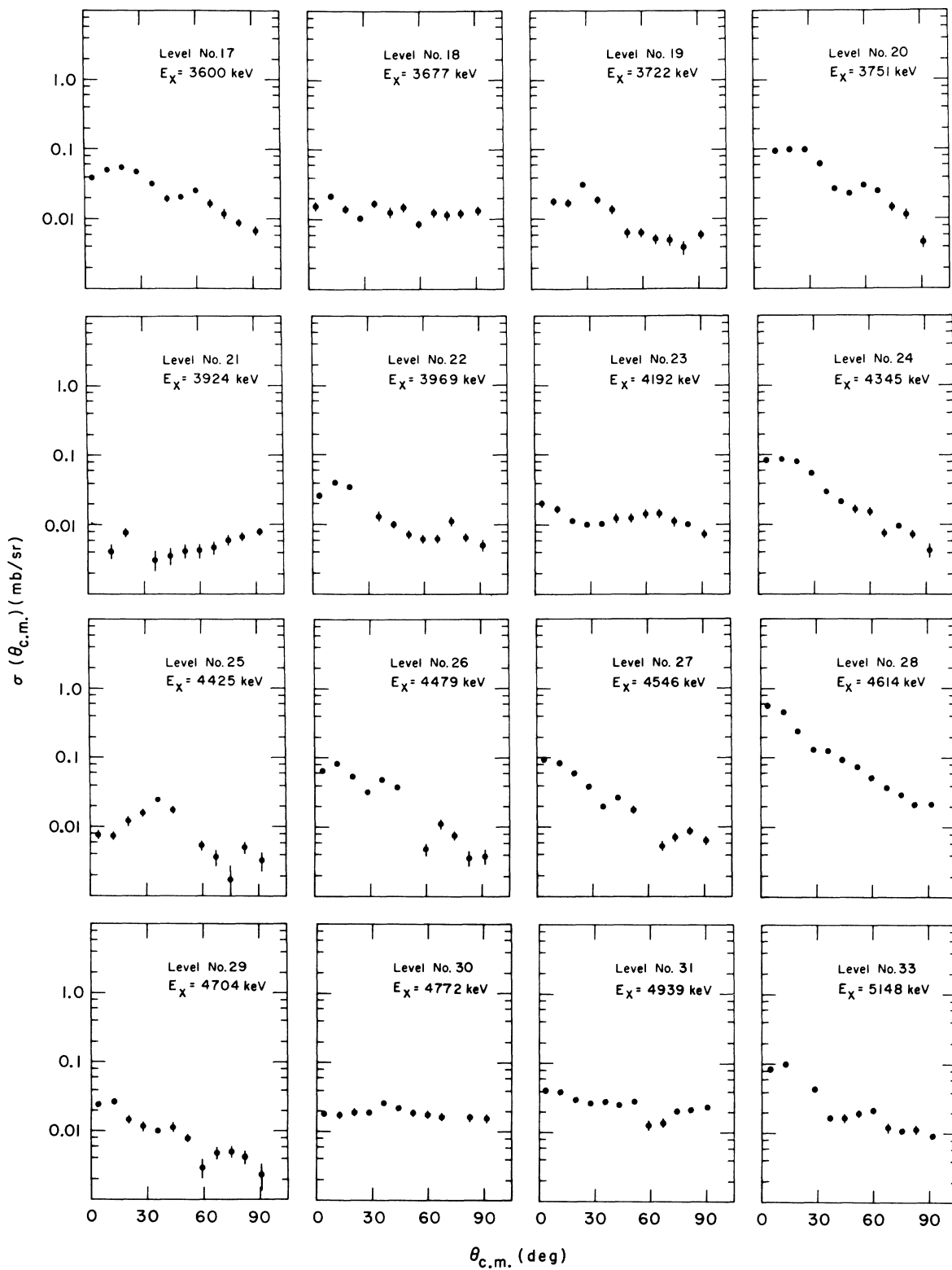


Fig. 2 (Continued).

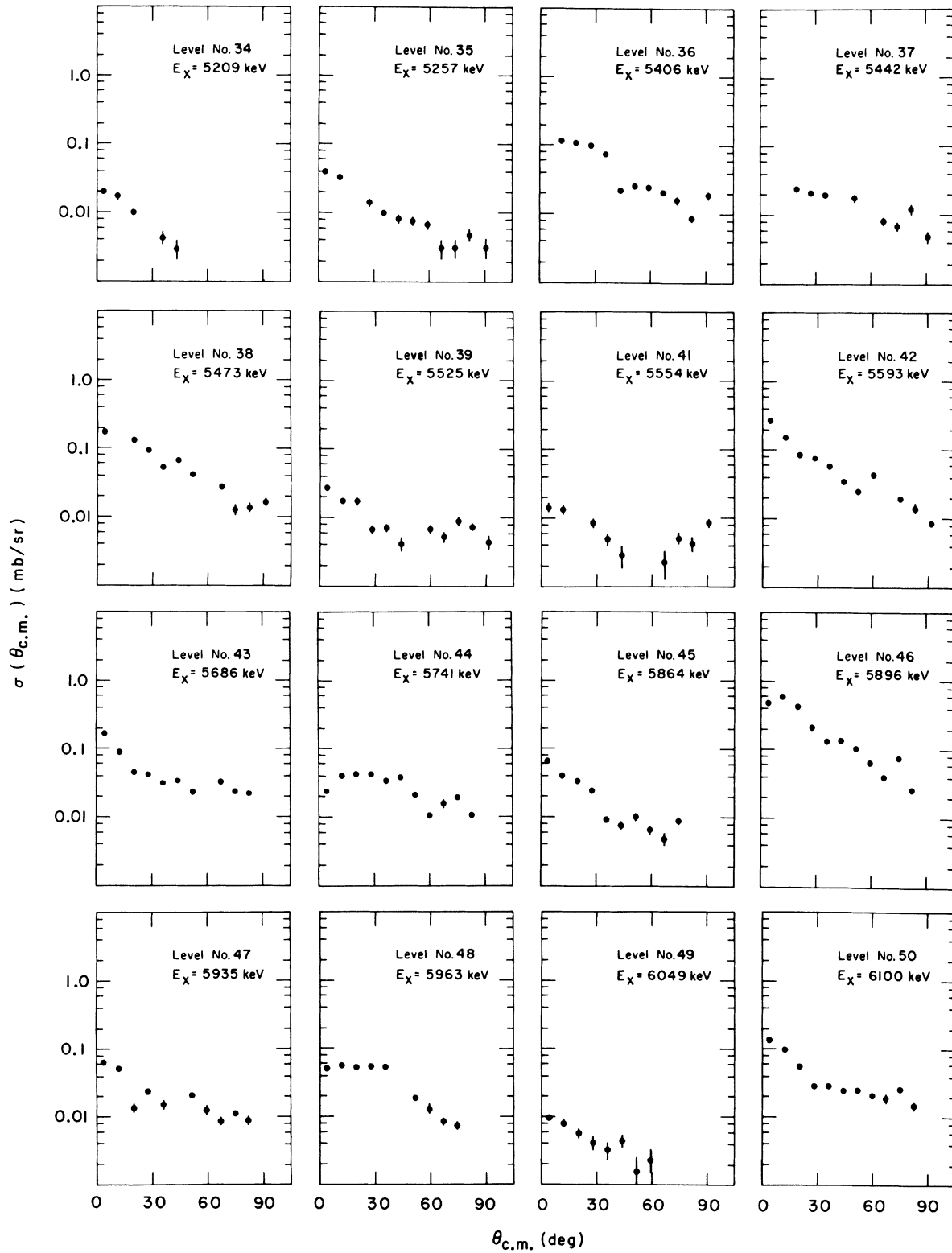


Fig. 2 (Continued).

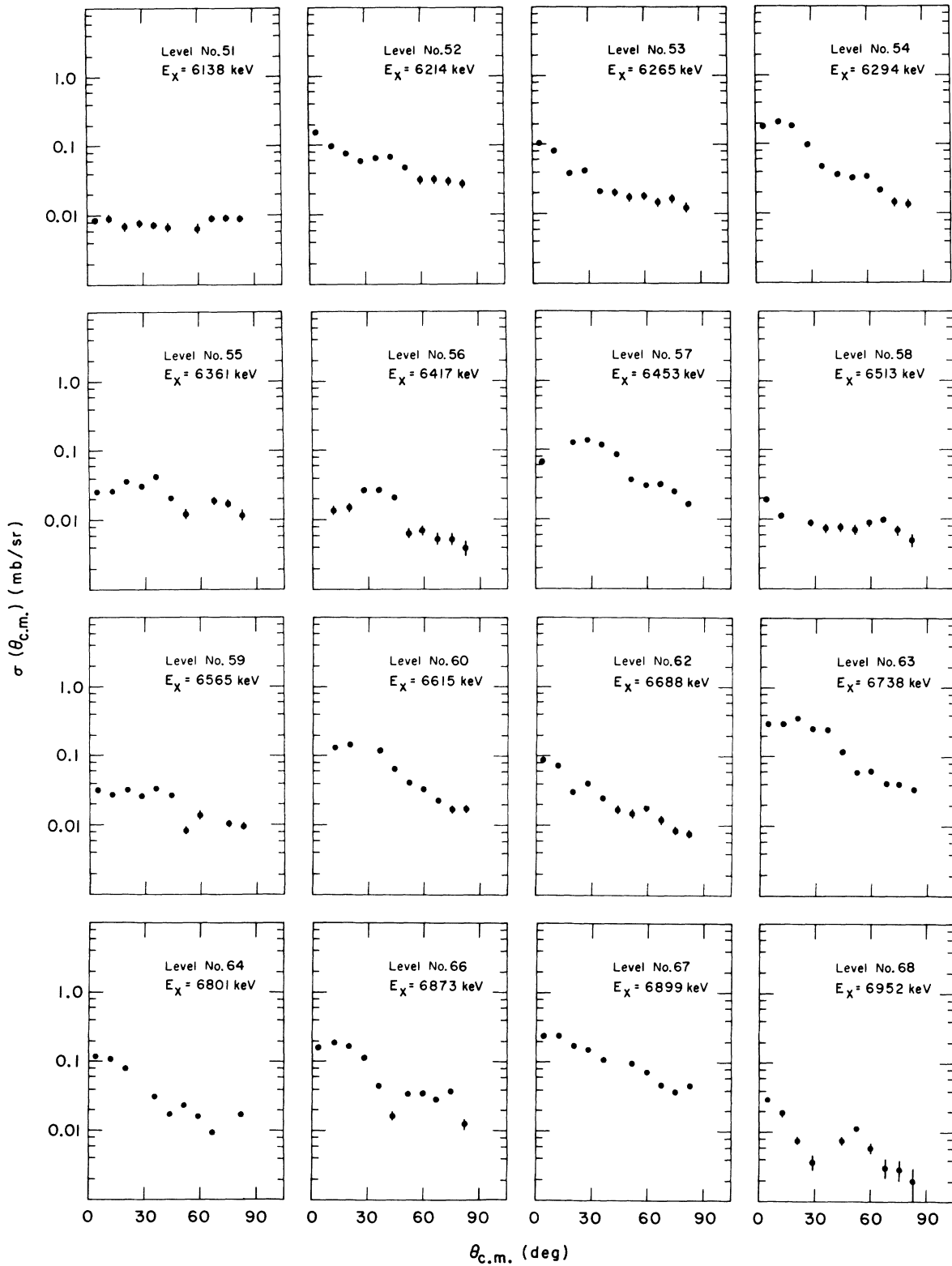


Fig. 2 (Continued).

not dominated by $L=0$ (Ref. 1). This would seem to cast some doubt on the previous $J=1$ assignment.

The angular distribution for the 3408-keV state does not have a characteristic $L=4$ shape, even though that state has recently been shown to have $J^\pi = 5^+$ (Scharpey-Schafer *et al.*¹⁹). The transition is, however, very weak and the state may be populated by processes other than direct two-particle stripping. Similarly, the transitions to the levels at 3507, 3677, and 3924 keV are also weak and the distributions are not characteristic of any single L value. This result is understandable for the 3507-keV state in view of its recent assignment¹⁹ of $J^\pi = 6^+$, since a 6^+ state in ^{26}Al cannot be populated directly by adding two sd -shell particles to the ^{24}Mg ground state. In the latter two cases, the observed result may be due to strong mixing between two L values which can result in a variety of angular-distribution shapes. This is most probably the case for the 3677-keV "level" since it has recently²⁰ been shown to be a closely spaced doublet.

The presence of an $L=0$ component in the distribution for the 3722-keV state requires $J^\pi = 0^+$ or 1^+ . In view of the observed γ decay of this state to the 224-keV 0^+ , $T=1$ state^{7,20} we can rule out spin zero, leaving only $J^\pi = 1^+$, $T=0$. An earlier assignment⁴ of 0^+ , $T=1$ to this state is in-

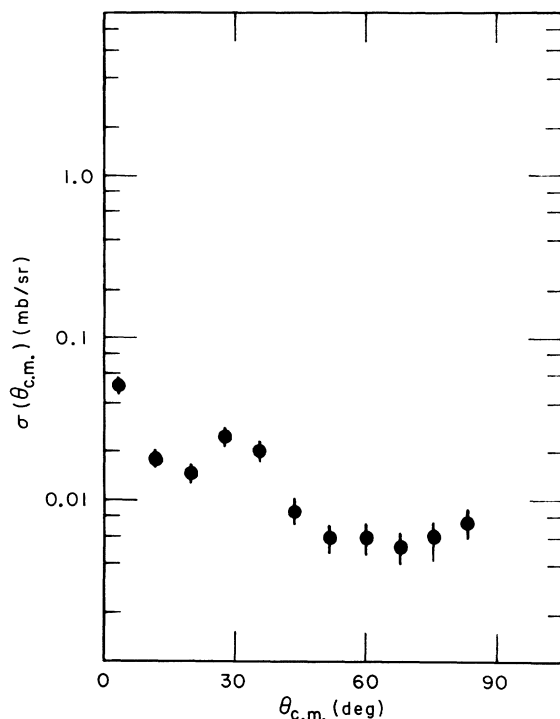


FIG. 3. Angular distribution for the 3722-keV state, measured at a bombarding energy of 19.5 MeV. (Level No. 19.)

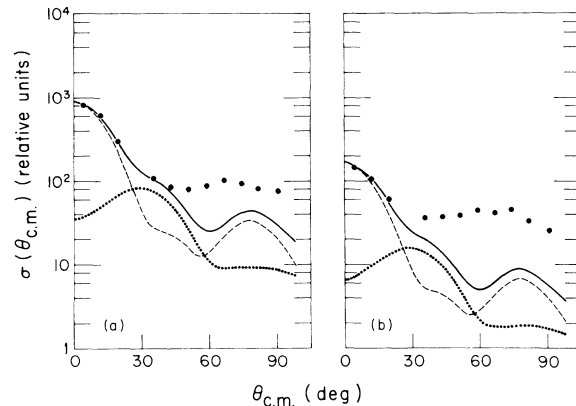


FIG. 4. Angular distributions for the reaction $^{24}\text{Mg}(^3\text{He}, p)^{26}\text{Al}$ for the (a) 3751- and (b) 3722-keV states, measured at a bombarding energy of 11 MeV. The dotted lines (\cdots) represent $L=2$ and the dashed lines ($---$) represent $L=0$. The curves are the results of distorted-wave calculations using the optical-model parameters given in Table III.

correct.

It has recently been determined²⁰ that the level observed at 3751 keV in the present study is in fact a closely spaced doublet. Unfortunately at both 18- and 19.5-MeV bombarding energy, this level was obscured at the most forward angle by a proton group leading to the first excited state of ^{14}N . A third exposure was thus made at an incident energy of 11 MeV. The angular distributions measured at 11 MeV for the 1^+ state at 3722 keV and for the 3751-keV doublet are shown in Fig. 4. The similarity of shapes indicates an $L=0$ component for the 3751-keV doublet. Since one member of this doublet has been assigned¹⁰ $J^\pi = (2, 3)^+$, the present results require $J^\pi = 0^+$ or 1^+ for the second member of the doublet. In fact, from all existing evidence, this state has been identified²⁰ as the second 0^+ , $T=1$ state in ^{26}Al - the analog of the 0^+ states at 3.59 MeV in ^{26}Mg and 3.35 MeV in ^{26}Si .

The angular distribution of the transition leading to the level at 4345 keV has a shape dominated by $L=2$, thus establishing a spin parity of 1^+ , 2^+ , or 3^+ for that state. The absence of $L=0$ would favor 2^+ or 3^+ .

A comparison of the ground-state "standard"

TABLE II. Macroscopic selection rules for the $(^3\text{He}, p)$ reaction on a 0^+ , $T=0$ target.

J_f	π_f	T_f	L	S	T
0	+	1	0	0	1
>0	$(-1)^{J_f}$	1	J_f	0	1
>0	$(-1)^{J_f}$	0	J_f	1	0
>0	$-(-1)^{J_f}$	0	$J_f \pm 1$	1	0

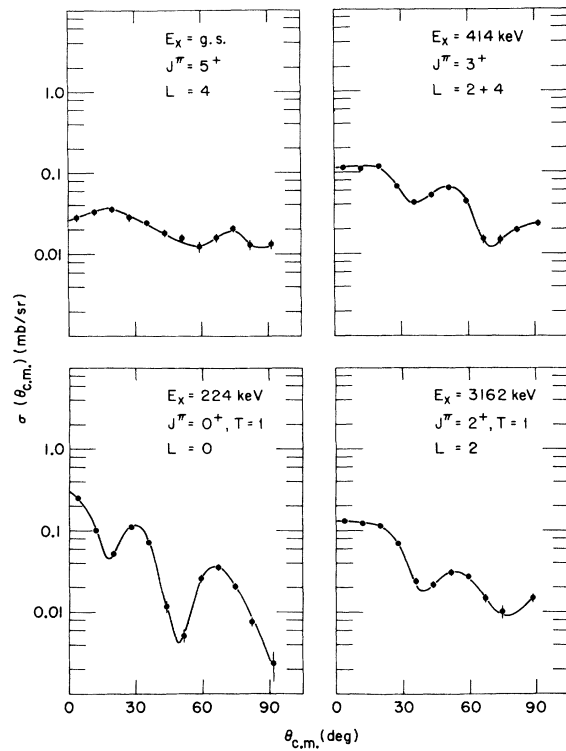


FIG. 5. "Standard" angular distributions for the $^{24}\text{Mg}-(^3\text{He}, p)^{26}\text{Al}$ reaction measured at $E(^3\text{He}) = 18.0$ MeV.

distribution with that of the transition to the 4425-keV level suggests an $L = 4$ assignment for the latter. Although there are dissimilarities in detail, both show a maximum cross section at an angle significantly greater than that for $L = 2$.

In view of the lack of other experimental information on the levels above 4.5 MeV in ^{26}Al , we have refrained from drawing any conclusions about the higher excited states. The main problem in the present experiment is the difficulty in distinguishing between, for example, strongly mixed $L = 0 + 2$ shapes and $L = 1$ shapes. Further analysis must await more information on the parities of the higher-lying levels. Angular distribu-

tions for these states, however, are also included in Fig. 2. A summary of L and J^π values for the levels below 4.5 MeV is given in Table I.

V. DISTORTED-WAVE ANALYSIS

Distorted-wave Born-approximation (DWBA) calculations were performed using the two-particle-transfer option of the code DWUCK.²¹ Optical-model parameters for the bound state, exit and entrance channels were taken from other work in this mass region²²⁻²⁴ and are listed in Table III. The code DWUCK calculates the two-particle form factor by taking the individual motions of both nucleons into account and projecting out the relative angular-momentum-zero part, according to the method described by Bayman and Kallio.²⁵

The depth of the bound-state well was adjusted to give the correct binding energy, as determined by the separation-energy procedure

$$B_n = B_p = \frac{1}{2} [Q(^3\text{He}, p) + E_{\text{sep}}],$$

where $E_{\text{sep}} = 7.72$ MeV for $S = 0$, $T = 1$ transfer and $E_{\text{sep}} = 5.54$ MeV for $S = 1$, $T = 0$ transfer. (The two different values of E_{sep} reflect the difference in energy of the singlet and triplet states of the deuteron.) In fact, the binding energy of the proton and neutron should be different because of the Coulomb energy. The effects of such a difference were investigated in several cases. Varying the neutron and proton binding energies while keeping their sum constant produced only very small (a few percent) changes in the shapes and magnitudes of the predicted angular distributions. Therefore the theoretical curves shown in Fig. 4 were calculated under the assumption of equal neutron and proton binding energies.

Although the predicted shapes of the angular distributions are not very sensitive to the final configurations, the magnitudes are. (See, e.g., Ref. 4.) Therefore, in order to obtain meaningful quantitative results from a distorted-wave analysis of two-particle-transfer reactions, a detailed know-

TABLE III. Optical-model parameters used in the distorted-wave analysis of the $^{24}\text{Mg}(^3\text{He}, p)^{26}\text{Al}$ reaction.

Channel	V (MeV)	$r_0 = r_{so}$ (fm)	$a = a_{so}$ (fm)	W (MeV)	$W' = 4W_D$ (MeV)	r'_0 (fm)	a' (fm)	V_{so} (MeV)	r_{0c} (fm)
$^{24}\text{Mg} + ^3\text{He}^a$	177.0	1.138	0.724	10.0	0	1.602	0.796	4	1.29
$^{26}\text{Al} + p^b$	55.18	1.128	0.57	...	33.14	1.128	0.50	5.5	1.13
Bound state ^c	d	1.26	0.60	$\lambda = 25$	1.26

^a Reference 23.

^b Reference 24. The set shown is for the ground state. The Q dependence used is that given in the reference.

^c Reference 22.

^d Adjusted to give the binding energy $B_n = B_p = 1/2(Q + E_{\text{sep}})$ where $E_{\text{sep}} = 5.54$ MeV for $T = 0$ transfer and $E_{\text{sep}} = 7.72$ MeV for $T = 1$ transfer.

ledge of the wave functions is essential. Since ^{26}Al lies in a region of nuclei known to be deformed, several attempts^{10,12} have been made to describe its level scheme in terms of two particles moving in a deformed potential relative to a ^{24}Mg core. The validity of such an interpretation can readily be tested by means of the $^{24}\text{Mg}(^3\text{He}, p)$ reaction, since those states well described by this model are expected to be strongly excited in a direct transfer of the two nucleons.

Two-particle coefficients of fractional parentage (cfp) have been calculated within the framework of the Nilsson model, according to the procedure described in Ref. 2. The coefficients in the expansion of the Nilsson eigenfunctions in terms of shell-model wave functions were taken from the work of Chi.²⁶ The low-lying states of ^{26}Al are expected in this model to be formed by placing two particles in Nilsson orbits No. 5, $\frac{5}{2}^+[202]$; No. 9, $\frac{1}{2}^+[211]$; No. 11, $\frac{1}{2}^+[200]$; or No. 8, $\frac{3}{2}^+[202]$, as indicated schematically in Fig. 6.²⁷ The single-nucleon transfer^{10,11} and charge-exchange²⁸ reactions enable those states with dominant configurations of the form $(\frac{5}{2}^+[202] \times K^\pi[Nn_z \Lambda])_{J^\pi}$ to be identified. The states so identified are listed in Table IV, together with the calculated cfp's as a function of

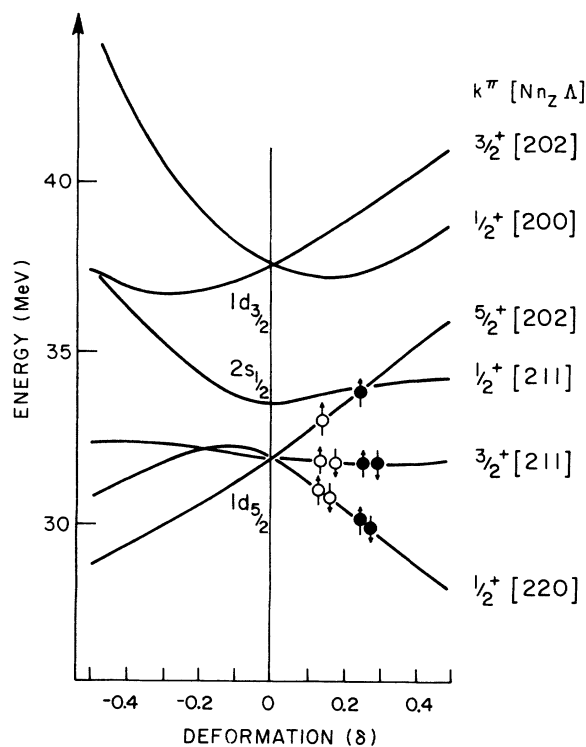


FIG. 6. Nilsson diagram showing sd -shell orbitals as a function of deformation. The filled orbitals depict the supposed dominant configuration of the ^{26}Al ground state. Solid dots (\bullet) are protons; circles (\circ) are neutrons.

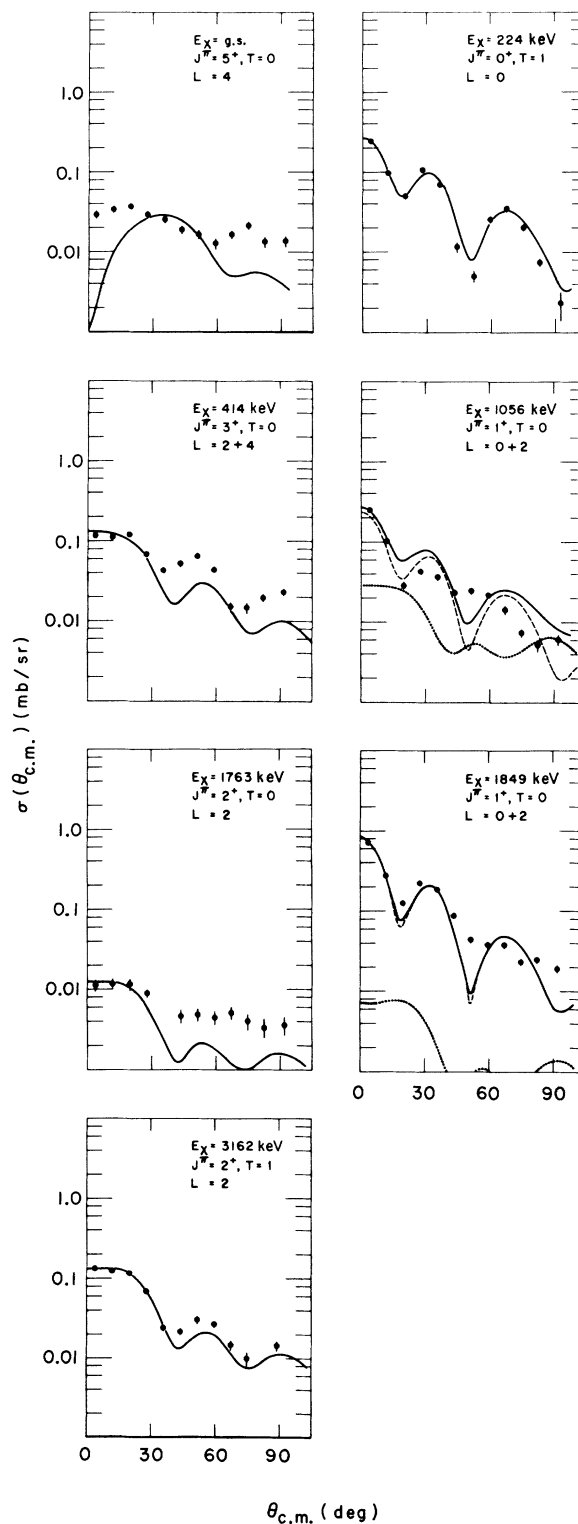


FIG. 7. Distorted-wave fits to the data for certain low-lying states. The calculations were made with the cfp's listed in Table IV for $\delta = 0.2$.

the deformation δ . It should be noted that for the configuration $(\frac{5}{2}^+ [202])_{\pi, \kappa}^2$ the coefficients are independent of the value of δ , whereas for other configurations the coefficients are strongly dependent on the deformation.

Figure 7 shows the results of DWBA calculations with the coefficients of fractional parentage determined for a deformation $\delta = 0.2$. The pure $L = 0$ calculation for the 224-keV state ($J^\pi = 0^+$, $T = 1$) is in excellent agreement with the experimental angular distribution for that state. Agreement is also excellent for the 2^+ , $T = 1$ state at 3162 keV, which must be reached via pure $L = 2$ transfer. The fits to the 2^+ , $T = 0$ state at 1763 keV and the 5^+ ground state are, however, must less satisfactory. Since these states are only weakly excited in this reaction, the poor fits may indicate the presence of higher-order reaction mechanisms.

The remaining states whose angular distributions are displayed in Fig. 7 are all of unnatural parity, and are hence populated by a mixture of two L values. In none of these cases is the fit as good as for the strong, pure L cases, although the agreement at extreme forward angles is quite acceptable. This inability to reproduce the shapes of mixed- L angular distributions has been noted previously,² particularly for the case of $0^+ \rightarrow 1^+$ transitions. It has been suggested² that the difficulty might be due

to a coherent mixing between the two allowed L values. Since the introduction of spin-orbit potentials in the entrance and exit channels makes the sum over L in the transition amplitudes necessarily coherent,²⁹ the code DWUCK has been modified³⁰ to perform this coherent sum. The differences between a coherent and incoherent sum are shown in Fig. 8 for the 1.06-MeV $0^+ \rightarrow 1^+$ transition. The change due to coherence is slight and is insufficient to account for the observed shapes. The reason for this consistent failure to fit $0^+ \rightarrow 1^+$ angular distributions is not understood and is under further investigation. It should be noted that *no* admixture of $L = 0$ and $L = 2$ will fit these angular distributions.

For a ($^3\text{He}, p$) reaction on a spin-zero target, the experimental cross section is related to the cross section calculated with the code DWUCK through the relation

$$\sigma_{\text{exp}} = NC^2 \sigma_{\text{DWUCK}}.$$

If, in addition, the target has zero isospin, the isospin Clebsch-Gordan coefficient C is the same for both $T = 0$ and $T = 1$ final states. There is no reason to assume *a priori* that the quantity N , which includes the overlap between the projectile and the transferred "cluster" and outgoing proton, has the same value for $T = 0$ and $T = 1$ transfer.

TABLE IV. Two-particle coefficients of fractional parentage calculated within the framework of the Nilsson model.

E_x (MeV)	J^π, T	K	Nilsson configuration	δ	$1d_{5/2}$	$1d_{5/2}$	$1d_{3/2}$	$1d_{3/2}$	$2s_{1/2}$	$2s_{1/2}$	$1d_{5/2}$	$1d_{3/2}$	$1d_{5/2}$	$2s_{1/2}$ ^a	$1d_{3/2}$	$2s_{1/2}$ ^a		
0.00	$5^+, 0$	5	$\frac{5}{2}^+ [202] \times \frac{5}{2}^+ [202]$	0.1	0.852	0.80												
				0.2	0.852	0.80												
				0.3	0.852	0.80												
0.23	$0^+, 1$	0	$\frac{5}{2}^+ [202] \times \frac{5}{2}^+ [202]$	0.1	0.816	0.50												
				0.2	0.816	0.50												
				0.3	0.816	0.50												
0.42	$3^+, 0$	3	$\frac{5}{2}^+ [202] \times \frac{1}{2}^+ [211]$	0.1	0.232	0.61					0.179	0.36	0.805	0.85				
				0.2	0.287	0.60						0.286	0.41	0.529	0.23			
				0.3	0.306	0.04						0.318	0.41	0.370	0.42			
1.06	$1^+, 0$	0	$\frac{5}{2}^+ [202] \times \frac{5}{2}^+ [202]$	0.1	0.690	0.07												
				0.2	0.690	0.07												
				0.3	0.690	0.07												
1.76	$2^+, 0$	2	$\frac{5}{2}^+ [202] \times \frac{1}{2}^+ [211]$	0.1							0.185	0.25	0.465	0.26				
				0.2								0.295	0.81	0.305	0.55			
				0.3								0.328	0.86	0.213	0.86			
1.85	$1^+, 0$	0	$\frac{1}{2}^+ [211] \times \frac{1}{2}^+ [211]$	0.1	0.023	0.52	-0.046	0.52	0.530	0.23								
				0.2	0.035	0.96	-0.118	0.61	0.228	0.69								
				0.3	0.040	0.72	-0.146	0.60	0.112	0.03								
3.16	$2^+, 1$	2	$\frac{5}{2}^+ [202] \times \frac{1}{2}^+ [211]$	0.1	0.220	0.67					0.185	0.25	0.465	0.26				
				0.2	0.272	0.83						0.295	0.81	0.305	0.55			
				0.3	0.290	0.33						0.328	0.86	0.213	0.86			

^a The phase convention of the wave functions used in the code DWUCK differs from that of Chi. The cfp's for $2s_{1/2}-1d_{5/2}$ and $2s_{1/2}-1d_{3/2}$ configurations should be multiplied by (-1) for use in the code.

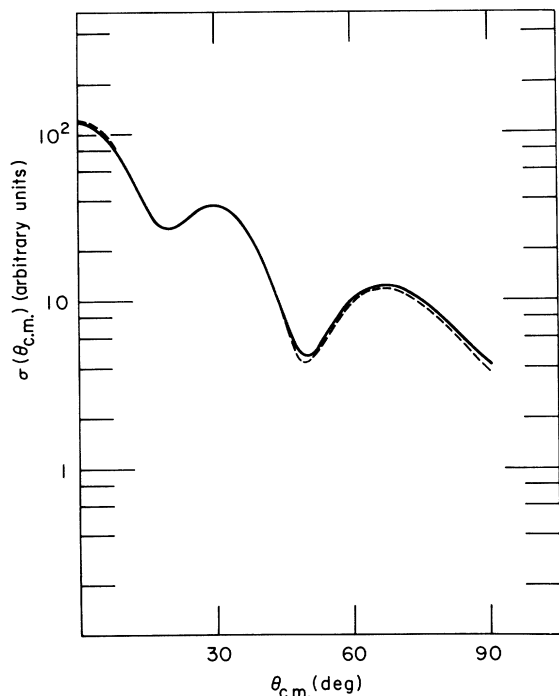


FIG. 8. Comparison between a coherent and incoherent sum of $L=0$ and 2 for the $J^\pi=1^+$ state at 1.06 MeV. The solid (—) line represents the coherent sum and the dashed (---) line the incoherent sum.

However, if the exact final (and initial) wave functions are the same as those used in the DWBA calculations, then the values of the quantity $\sigma_{\text{exp}}/\sigma_{\text{DWUCK}}$ should be the same for all states having the same T . Table V lists the values of $\sigma_{\text{exp}}/\sigma_{\text{DWUCK}}$ obtained from the present calculations as a function of deformation. The large variation of this quantity from state to state, for all values of the deformation used, indicates the inadequacy of the present description of ^{26}Al . The agreement is equally poor for all values of the deformation. It is known that

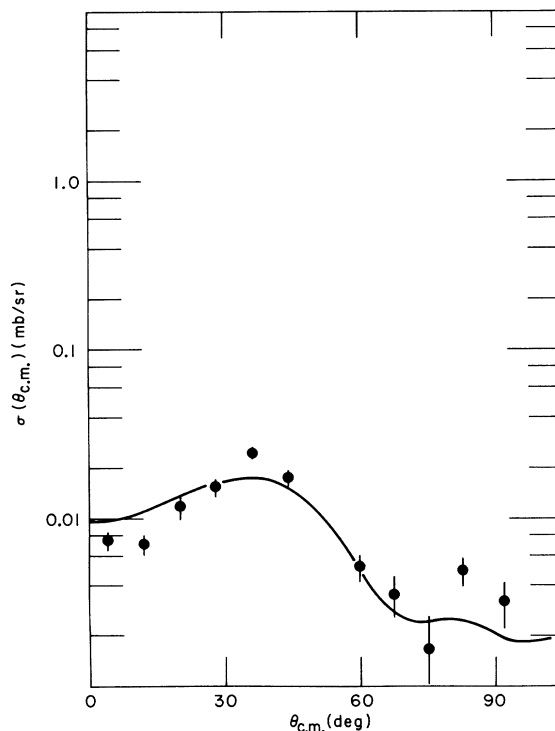


FIG. 9. $L=4$ DWBA fit to the angular distribution for the 4425-keV state.

small admixtures in the final-state wave functions can drastically change the magnitude of the predicted cross sections. The simple Nilsson picture, however, is clearly unsatisfactory and a more detailed DWBA analysis must await a sophisticated shell-model calculation or a full Nilsson-type calculation with band mixing.

In view of these difficulties, no detailed DWBA analysis was attempted for the remaining states. A calculation using a simple form factor was performed, however, for the state at 4425 keV, the

TABLE V. Values of $\sigma_{\text{exp}}/\sigma_{\text{DWUCK}}$ obtained from the DWBA analysis of the $^{24}\text{Mg}(^3\text{He}, p)^{26}\text{Al}$ reaction for selected states.

Level E_x (MeV)	J^π, T	Assumed configuration	$\sigma_{\text{exp}}/\sigma_{\text{DWUCK}}$		
			$\delta=0.1$	$\delta=0.2$	$\delta=0.3$
0.00	$5^+, 0$	$(\frac{5}{2}^+ [202] \times \frac{5}{2}^+ [202]) K=5$	10	10	10
0.23	$0^+, 1$	$(\frac{3}{2}^+ [202] \times \frac{5}{2}^+ [202]) K=0$	129	129	129
0.42	$3^+, 0$	$(\frac{5}{2}^+ [202] \times \frac{1}{2}^+ [211]) K=3$	11	24	46
1.06	$1^+, 0$	$(\frac{5}{2}^+ [202] \times \frac{5}{2}^+ [202]) K=0$	234	234	234
1.76	$2^+, 0$	$(\frac{5}{2}^+ [202] \times \frac{1}{2}^+ [211]) K=2$	8	11	14
1.85	$1^+, 0$	$(\frac{1}{2}^+ [211] \times \frac{1}{2}^+ [211]) K=0$	178	780	2361
3.16	$2^+, 1$	$(\frac{5}{2}^+ [202] \times \frac{1}{2}^+ [211]) K=2$	23	33	46

result is shown in Fig. 9. The good agreement between experimental and theoretical shapes gives further indication that this state is indeed populated via $L=4$, thus resulting in $J^\pi = 3^+, 4^+$, or 5^+ . The absence of any $L=2$ component, however, would favor either 4^+ or 5^+ .

DWBA angular distributions were also calculated for the 3722- and 3751-keV states at 11-MeV incident energy and these are shown in Fig. 4. The calculations clearly show that the forward-angle data are dominated by $L=0$ components, as discussed previously (Sec. IV).

VI. CONCLUSIONS

The ($^3\text{He}, p$) reaction is known to be a useful empirical spectroscopic tool. The systematics of the angular-distribution shapes for the $^{24}\text{Mg}(^3\text{He}, p)$ - ^{26}Al reaction has allowed the identification of L values for a number of transitions and has led to spin and parity assignments for several levels in ^{26}Al .

DWBA calculations are reasonably successful in accounting for the observed angular-distribu-

tion shapes. The previously observed discrepancy between the measured and calculated distributions for 1^+ states is also observed in the present study. In addition, it has been shown that coherent mixing between the two allowed L values in such cases does not account for this discrepancy – at least within the assumptions of a simple direct one-step transfer.

Finally, the simple picture of ^{26}Al as two nucleons moving in a deformed well formed by a ^{24}Mg core is unable to account for the present data. This points to the need for more sophisticated shell-model calculations for ^{26}Al .

ACKNOWLEDGMENTS

We are grateful to Lois Ballard for her careful scanning of the nuclear emulsion plates. We also thank T. Caldwell and P. Neogy for their assistance in the data accumulation. It is a pleasure to acknowledge interesting and informative discussions with J. W. Noé, G. A. Bissinger, and P. R. Chagnon. Our thanks are also due to Laszlo Csihas for his careful preparation of the targets.

*Work supported by the National Science Foundation.

¹R. R. Betts, H. T. Fortune, J. D. Garrett, R. Middleton, D. J. Pullen, and O. Hansen, *Phys. Rev. Letters* **26**, 1121 (1971).

²J. D. Garrett, R. Middleton, D. J. Pullen, S. A. Andersen, O. Nathan, and O. Hansen, *Nucl. Phys.* **A164**, 449 (1971).

³H. T. Fortune, J. D. Garrett, J. R. Powers, and R. Middleton, *Phys. Rev. C* **4**, 850 (1971).

⁴H. T. Fortune, R. R. Betts, P. Neogy, and D. J. Pullen, *Phys. Letters* **36B**, 3 (1971).

⁵S. Hinds and R. Middleton, *Proc. Roy. Soc. (London)* **73**, 501 (1959).

⁶G. A. Bissinger, P. A. Quin, and P. R. Chagnon, *Nucl. Phys.* **A115**, 33 (1969).

⁷G. A. Bissinger, P. A. Quin, and P. R. Chagnon, *Nucl. Phys.* **A132**, 529 (1969).

⁸O. Häusser and N. Anyas-Weiss, *Can. J. Phys.* **46**, 2809 (1968).

⁹O. Häusser, T. K. Alexander, and C. Broude, *Can. J. Phys.* **46**, 1035 (1968).

¹⁰A. Weidinger, R. H. Siemssen, G. C. Morrison, and B. Zeidman, *Nucl. Phys.* **A108**, 547 (1968).

¹¹H. Fuchs, K. Grabisch, P. Kraaz, and G. Roschert, *Nucl. Phys.* **A110**, 65 (1968).

¹²P. Horvat, P. Kump, and B. Povh, *Nucl. Phys.* **45**, 341 (1963).

¹³M. C. Bouten, J. P. Elliot, and J. A. Pullen, *Nucl. Phys.* **A97**, 113 (1967).

¹⁴P. Wasielewski and F. B. Malik, *Nucl. Phys.* **A160**, 113 (1971).

¹⁵T. Caldwell and N. Al-Jadir, University of Pennsylvania (unpublished).

¹⁶J. H. E. Mattauch, W. Thiele, and A. H. Wapstra, *Nucl. Phys.* **69**, 1 (1965).

¹⁷P. M. Endt and C. Van der Leun, *Nucl. Phys.* **A108**, 1 (1967).

¹⁸C. E. Moss, C. Detraz, and C. S. Zaidins, *Nucl. Phys.* **A174**, 408 (1971).

¹⁹J. F. Scharpey-Schafer, D. C. Bailey, P. E. Carr, A. N. James, P. J. Nolan, and D. A. Viggars, *Phys. Rev. Letters* **27**, 1463 (1971).

²⁰J. W. Noé, D. P. Balamuth, R. R. Betts, H. T. Fortune, and R. W. Zurmühle, *Nucl. Phys.* **A186**, 15 (1972).

²¹P. D. Kunz, University of Colorado (unpublished).

²²H. T. Fortune, T. J. Gray, W. Trost, and N. R. Fletcher, *Phys. Rev.* **179**, 1033 (1969).

²³H. T. Fortune, N. G. Puttaswamy, and J. L. Yntema, *Phys. Rev.* **185**, 1546 (1969).

²⁴B. A. Watson, P. P. Singh, and R. E. Segel, *Phys. Rev.* **182**, 977 (1969).

²⁵B. F. Bayman and A. Kallio, *Phys. Rev.* **156**, 1121 (1967).

²⁶B. E. Chi, *Nucl. Phys.* **83**, 97 (1966).

²⁷S. G. Nilsson, *Kgl. Danske Videnskab. Selskab, Mat.-Fys. Medd.* **29**, No. 16 (1955).

²⁸T. H. Curtis, H. F. Lutz, D. W. Heikkinen, and W. Bartolini, *Nucl. Phys.* **A154**, 293 (1970).

²⁹D. G. Fleming, J. Cerny, and N. K. Glendenning, *Phys. Rev.* **165**, 1153 (1968).

³⁰R. R. Betts, Ph.D. thesis, University of Pennsylvania, 1972 (unpublished).